Supporting Information

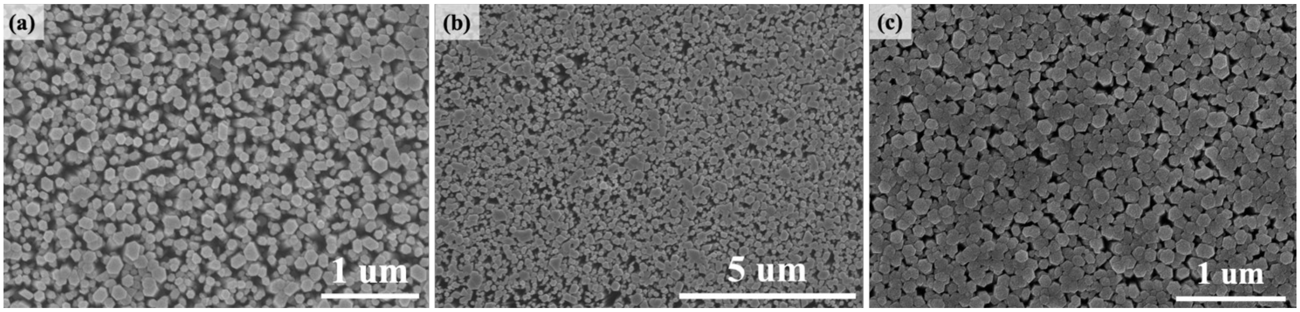

Figure S1. SEM images showing the morphology of the ZnO nanorods synthesized using different HMTA and $Zn(NO_3)_2$ precursor concentrations of (a) 0.02M, (b) 0.03M, and (c) 0.05M with the concentrations of HMTA and $Zn(NO_3)_2$ were kept equal as 1:1 volume ratio.

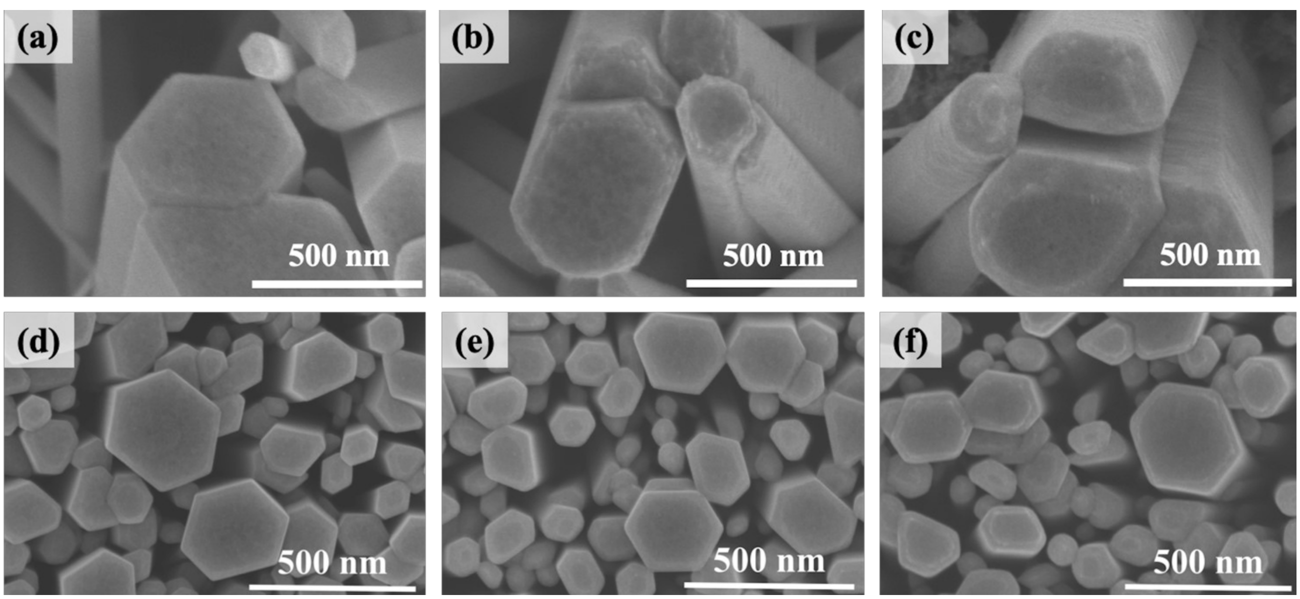

Figure S2. SEM images showing the morphology of the ZnO nanorods after Cu doping using different concentrations of $Cu(NO_3)_2$ precursor: (a) 0.01 M, (b) 0.02 M, and (c) 0.2 M; and different immersion times in 0.01 M $Cu(NO_3)_2$ solution: (d) 2 min, (e) 4 min, and (f) 6 min.

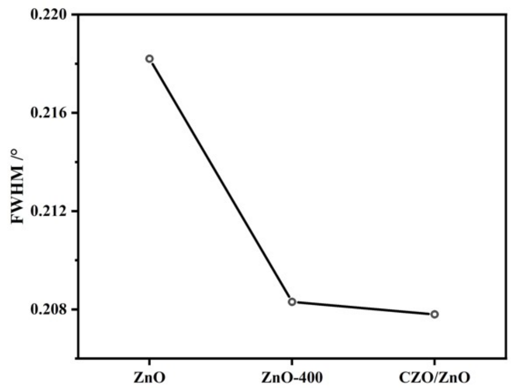

Figure S3. Variation in the FWHM values of the (002) diffraction peak for ZnO, ZnO-400, and CZO/ZnO samples.

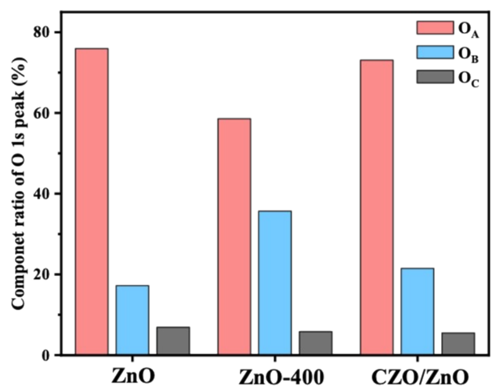

Figure S4. Fractions of different oxygen-related chemical states (O_A:lattice oxygen, O_B: oxygen vacancy, O_C: loosely bound surface oxygen) determined from O 1s XPS peak deconvolution in Figure 2(c) for ZnO, ZnO-400, and CZO/ZnO.

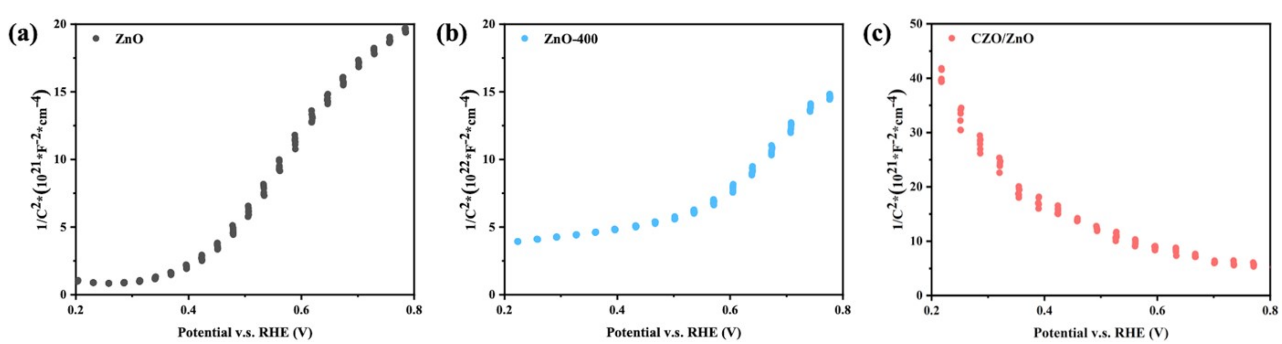

Figure S5. Mott-Schottky analysis of (a) ZnO, (b) ZnO-400, and (c) CZO/ZnO

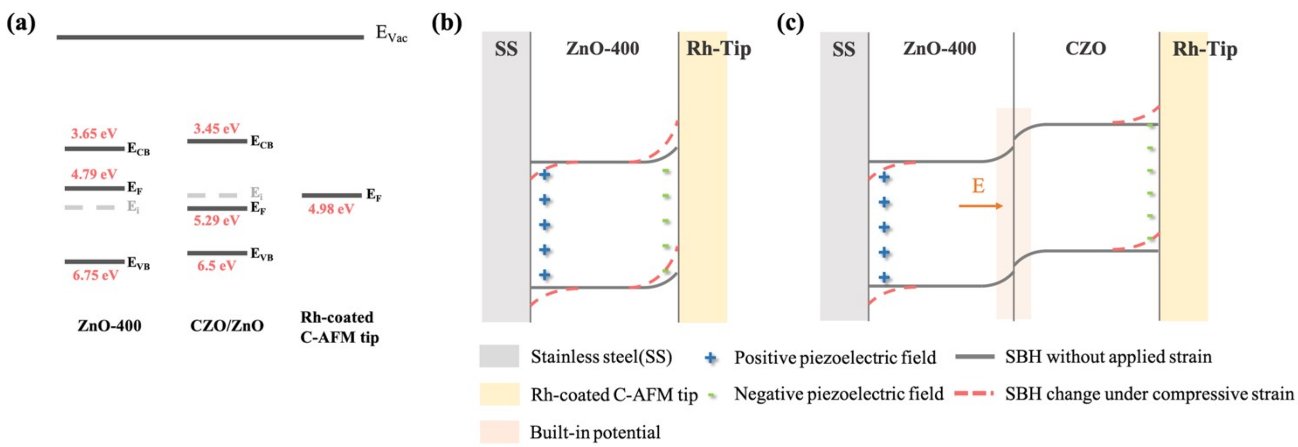

Figure S6. (a) Energy band structure of ZnO-400 and CZO/ZnO derived from UPS and UV-Vis measurements along with the E_F of the Rh-coated C-AFM tip. Schematic energy band diagrams of the (b) ZnO-400, and (c) CZO/ZnO under applied compressive force through the Rh-coated C-AFM tip.

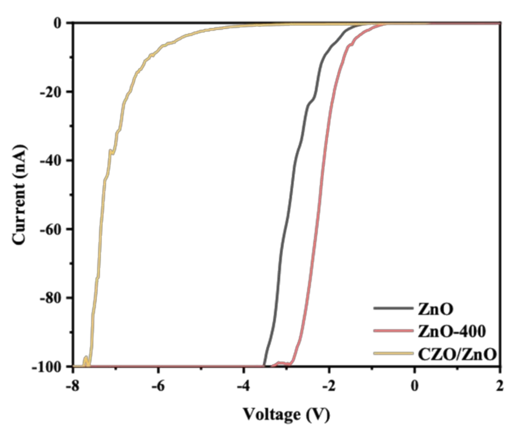

Figure S7. Current–voltage characteristics of (a) ZnO, (b) ZnO-400, and (c) CZO/ZnO under a compressive force of 20 nN.

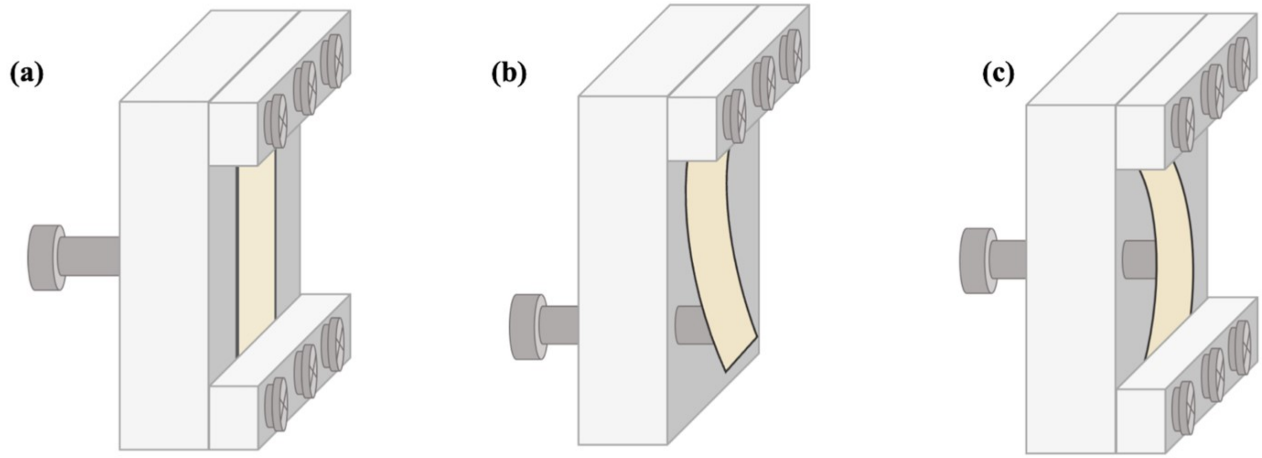

Figure S8. Schematic of the force applicator for (a) no applied stress, (b) applied compressive stress, and (c) applied tensile stress.

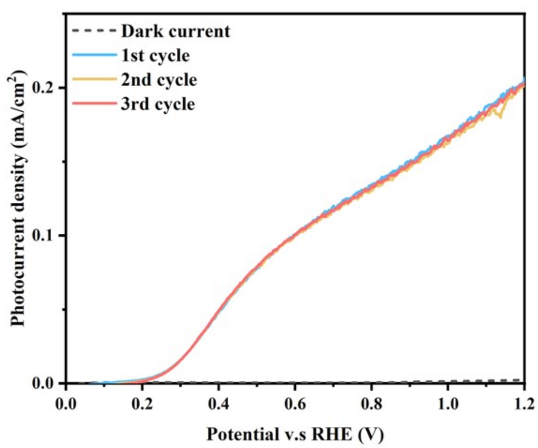

Figure S9. PEC performance repeatability test of ZnO under compressive strain (ε=-0.15%).

Structure	Electrolyte	Mechanical Force	Light Intensity	*J* of pristine ZnO without Strain (mA/cm^2, 1.23 V_{RHE})	*J* of modification ZnO with Strain (mA/cm^2, 1.23 V_{RHE})	Enhancement Factor	Ref.
Dual cocatalysts-ZnO	0.1 M Na_2SO_4 with 0.1 M K_3PO_4 solution (pH = 7.0)	Ultrasonic vibration (90kHz), ε=Not specified	$100mW/cm^2$	0.27	0.8	2.96	[1]
Asymmetric Au-ZnO NRs	0.5M Na_2SO_4 solution (pH = 7.0)	Ultrasonic vibration (80W, 40kHz), ε=Not specified	$100mW/cm^2$	0.054	0.185	3.42	[2]
ZnO nanosheets/ MoS_2 heterostructure	0.1 M Na_2SO_4 solution (pH = 7.0)	Ultrasonic vibration, ε=Not specified	$100mW/cm^2$	0.1	0.68	6.8	[3]
ZnO-WO_{3-x} NRs	1 M Na_2SO_4 solution (pH = 7.0)	Magnetic bar stirring (1000RPM), ε=Not specified	$100mW/cm^2$	1.12	3.38	3.02	[4]
2 at% Sb-doped ZnO NRs	0.1 M Na_2SO_4 solution (pH = 7.0)	Bending, $\varepsilon = 1.5 \times 10^{-3}$ (tensile strain)	$100mW/cm^2$	0.54	1.37	2.53	[5]
Porous core-shell ZnO p-n homojunction	0.1 M Na_2SO_4 solution (pH = 7.0)	$\varepsilon = -1.5 \times 10^{-3}$ (compressive strain)	$100mW/cm^2$	0.18	0.71	3.94	This work

Table S1. Comparative analysis of photocurrent density and enhancement factors for ZnO-based materials under mechanical strain. Enhancement factor is calculated as the ratio of photocurrent density with strain and modification ZnO to that of pristine ZnO without strain.

Reference

1. S. C. Zhang, Z. F. Liu, M. N. Ruan, Z. G. Guo, L. E, W. Zhao, D. Zhao, X. F. Wu and D. M. Chen, *Applied Catalysis B-Environmental*, 2020, **262**.
2. D. L. Xiang, Z. R. Liu, M. Q. Wu, H. H. Liu, X. D. Zhang, Z. Wang, Z. L. Wang and L. L. Li, *Small*, 2020, **16**.
3. D. Wang, Q. Fu, J. Y. Tian, H. M. Zhou, R. Liu, D. F. Zhan, Z. Peng and C. C. Han, *Journal of Colloid and Interface Science*, 2024, **653**, 1166-1176.
4. Y. Chen, L. Wang, R. J. Gao, Y. C. Zhang, L. Pan, C. Y. Huang, K. Liu, X. Y. Chang, X. W. Zhang and J. J. Zou, *Applied Catalysis B-Environmental*, 2019, **259**.
5. Y. L. Hsiao, P. C. Chen, K. Gupta, C. C. Lai, Y. C. Pu and C. P. Liu, *Mrs Energy & Sustainability*, 2022, **9**, 19-27.